International Journal of Computer Sciences and Engineering
Vol.**11**, Issue **4**, pp.**30-38**, April **2023**
ISSN: 2347-2693 (Online)
Available online at: www.ijcseonline.org

ISSN: 2347-2693 (E)

Research Paper

Seed Selection for Region-Growing Image Segmentation Based on Detected Keypoints

Ibrahim El rube`[1]

[1]Computer Engineering Department, CIT College, Taif University, Taif, KSA

Author's Mail Id: Ibrahim.ah@tu.edu.sa

Received: 02/Mar/2023; **Accepted**: 10/Apr/2023; **Published**: 30/Apr/2023. | **DOI**: https://doi.org/10.26438/ijcse/v11i4.3038

Abstract: Seeded region growing (SRG) segmentation is utilized frequently in image processing, computer vision, and machine intelligence applications. The accuracy of the segmentation produced by the fundamental SRG algorithm relies on the proper seed selection. In this paper, seeds are allocated for each color component of the input image using a keypoint detector. Two methods for obtaining seeds are examined; the first method uses the keypoints as the seeds, while the second method uses the centers of the triangles constructed using the keypoints as the seeds for the SRG algorithm. After that, each color plane is subjected to the SRG algorithm, and the result is then concatenated. Subsequently, this segmentation is enhanced by employing a statistical region-merging algorithm. Several traditional keypoint detectors, such as SIFT, SURF, KAZE, and Harris, are compared and examined using the well-known Berkeley segmentation dataset (BSD) images. Finally, the provided technique is compared with two other approaches for image segmentation: K-means and mean shift.

Keywords: Region growing, seeds, image segmentation, keypoints detector, triangulations centers

1. Introduction

Image segmentation aims to group pixels into distinctive and recognizable image regions, i.e., areas correlating to specific surfaces, objects, or natural portions of objects. It is a pre-processing step for applications such as biometrics, shape and object detection and recognition, and medical imaging [1],[2]. There are a variety of techniques for segmentation that can be found in the literature and have been proposed and utilized over the last few decades. These methods can be classified into thresholding, clustering-based, boundary-based, region-based, and hybrid methods [3], [4], [5]. Techniques that rely on region growing are superior to edge-based ones in noisy images where it is challenging to distinguish boundaries. Also, the seeded region growing (SRG) [6] is region-based, combining smaller subregions or individual images into bigger ones; it is a comparably fast technique and a parameter-tuning-free method. However, choosing a good seed that affects the SRG and produces efficient segmentation still has challenges with various choices and selection methods. Different techniques, such as thresholding, edges and centroids, neighbor's area, and fuzzy, were used in the literature to create seeds.

This article illustrates an automated method for finding seeds to feed the region-growing segmentation approach; it is carried out using the following steps: A typical keypoint detector is employed to identify the seeds. Next, the seeds for the segmentation procedure are determined using either the keypoints themselves or the central locations of the triangles created by these keypoints. Consequently, an SRG segmentation algorithm is separately applied to each seed to obtain the segmented image. Statistical region merging (SRM) is then applied to the merged regions for additional processing.

The layout of the subsequent divisions is as follows: The next section briefly introduces related research on growing regions, the third section presents the proposed technique for growing regions-based segmentation, the fourth section demonstrates the experimental results, and lastly, the conclusion and recommendations for future research are presented in the final section.

2. Relate Work: Seeded Region Growing

2.1 Typical seeded region growing segmentation

Image segmentation utilizing seeded region growing algorithms can comprise the main stages shown in Figure 1. The input is usually a color/gray-level image followed by an optional pre-processing step with filtration and enhancements functions that the system developer specifies according to the condition of the input data. The first main procedure is to calculate the number and allocation of the seeds needed for the seeded region-growing (SRG) algorithm, which segments the image into similar regions accordingly. Usually, good segmentation results should be followed by a region merging (RM) algorithm that makes the overall segmentation process more meaningful with fewer metrics errors.

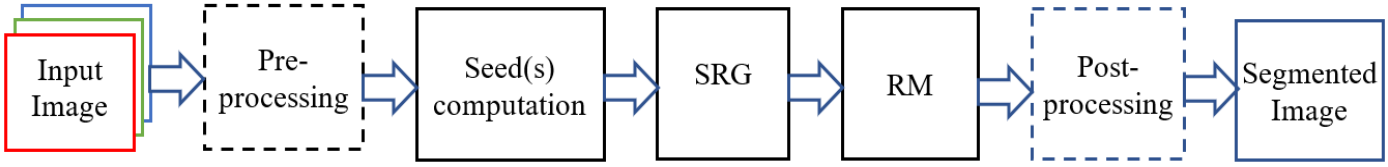

Figure 1. Typical SRG-based segmentation steps. The dashed-line blocks are non-compulsory.

The pre-processing and post-processing steps are usually embedded to enhance the results of the segmentation process. The exact operations in these two stages have yet to be agreed on across implementations, even for the same segmentation methods. However, it can vary according to several parameters, including the needed implementation requirements, the application domain specifications, the input data condition, and the shape and format of the desired results.

2.2 Region growing algorithms

Many region-growing segmentation methods and applications have been found in literature in recent decades. In [7], Watershed and Active Contour algorithms were used to evaluate the region-growing method for medical CT scans. The authors demonstrated that the proposed method segmented lung tumors effectively and may assist medical experts. A semi-automatic region-growing segmentation method with a progressive thresholding strategy based on probability maps and a unique Gray-Space map combining photo geometry and intensity levels was described in [8]. The authors recommend applying it outside medical imaging even though it is effective for parotid glands, tumors, and spinal cord segmentation. Region growing to utilize superpixels guided by previously acquired geometry information is presented in [9]. An innovative Smart Region Growth method (SmRG) for segmenting individual neurons in the complex 3D layout of the brain is presented in [10]. Its region-growing method uses a homogeneity criterion to recreate complex 3D cellular structures from high-resolution brain tissue photos. In [11], wave region-growing around local peaks were linked to close pixels in declining order of values to divide atomic force microscope images. In reference to flood monitoring applications, [12] compares and evaluates thresholding, region growing, and hybrid algorithms. According to tests, all methods can derive useful water information from images, but the hybrid strategy with high segmentation accuracy was the most effective. The authors of [13] offer a combined rough set and region-growing method to segment and identify fire smoke in images correctly. According to [14], segmentation of breast sonar images using an adaptive region growth technique based on a neutrosophic set (NSSRG) is suggested. By converting the photos into the NS domain, each pixel's similarity set score and uniformity value are computed to describe them. Seed regions are created using adaptive Otsu-based thresholding and shape.

Seeds can be selected manually or automatically generated by algorithms such as the local homogeneities, which include the J-image [15] and the H-image [16], the centroids between these adjacent edge regions [17], Harris corner detector [18], the similarity in a 3×3 pixel area with preset threshold values [19], rectangle centroids [20], color gradient and adaptive threshold [201], and fuzzy-based edge detection [22]. Automated SRG initial seed and cutoff value selection uses particle swarm optimization (PSO) cluster strengths in [23] for MRI breast tumors. Morphological thinning and level set active contour find and remove breast skin. In [19], a Harris corner detector is used after obtaining a single-color channel from multiple color mappings of the input image, then selecting one seed, and region-growing segmentation is applied. More recently, a non-parametric polygonal seed selection method enhances segmentation problem handling and seeded region growing (SRG) [24]. The proposed method offers a foundation for growing regions to improve medical imagery. Traditional SRG, K-Means, and Watershed segmentation provide qualitative data on axial brain slices. The seed-based region-growing method's early seed selection determines its partition in [25], where the local extreme pixels find the seed points. In [26], another SRG segmentation method used square areas instead of pixels for color images. The seeds were created using gradient values, and then RG and RM algorithms were applied. The study in [27] uses Advanced Complete Color Feature (ACCF) and Region growing process to divide disease-spotted leaves in real-world settings. Region growing removes debris backdrop in disease spot segmentation by directly choosing growing seeds in the ACCF map. In [28], the seeds are automatically selected from the pyramids of the Gaussian difference of images.

3. Keypoints-Based Region Growing Image Segmentation

As described earlier, seed computation is required for the SRG method to accomplish the segmentation process effectively. Often, the segmentation is performed on the grayscale version of the input image, as depicted in Figure 2 a), and seeds are frequently determined for the grayscale version of the input image. Therefore, in this scheme, which will be regarded as gray-level SRG (GSRG), the input image is first converted to the gray-level image to allocate the keypoints, then the strongest one(s) is selected as a seed(s) for the region-growing algorithm. Many traditional keypoints detectors exist in the literature, which can be used in this step, including SIFT [29], SURF [30], KAZE [31], Harris [32], and others. In the second scenario, as illustrated in Figure 2 b), the seeds are calculated independently for each color plane of the input image. The region growing is then applied to each color plane separately before using the SRM algorithm. Therefore, this scheme is regarded are color-image SRG (CSRG).

The segmentation procedure for GSRG, as depicted in Figure 2 a), will generate two segments per seed. If more image segments are desired, the segmentation procedure should utilize more seeds (i.e., robust keypoints). Increasing the number of seeds will improve the segmentation result at the expense of an increase in segmentation's overall computational time. For the CSRG in Figure 2 b), each color plane has its seeds that yield different segments; hence, for a single seed per color plane, the total number of segmentations after merging the three-color planes' results will range from two to eight. After region-growing segmentation, the statistical region merging (SRG) method enhances segmentation outcomes.

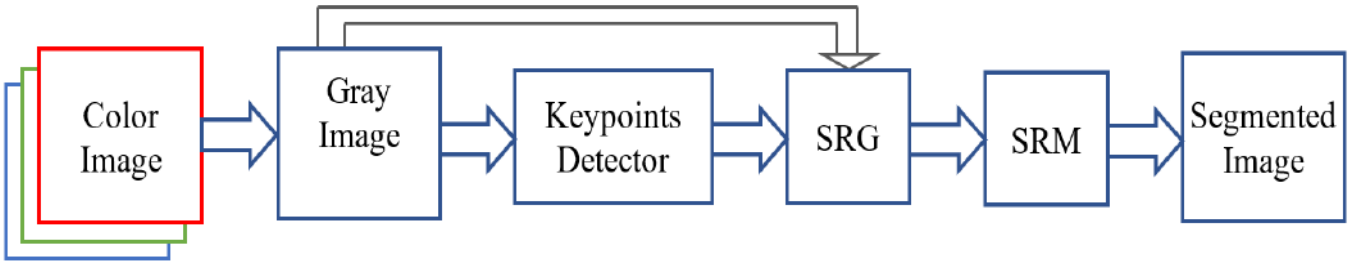

a) Gray-level image seeds computation with gray-image segmentation (GSRG).

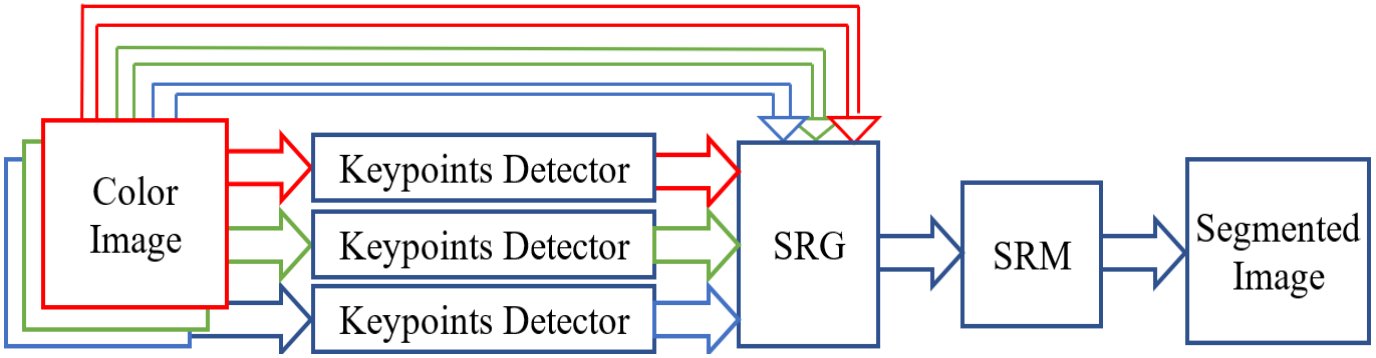

b) Color-image seeds computation with color-image segmentation (CSRG).

Figure 2. Image segmentation using seeded region growing; a) Gray-image based seeds with gray-image SRG segmentation (GSRG), b) Color-image channels-based seeds with Color-image SRG segmentation (CSRG).

To allocate the seeds for both cases, two methods are investigated. In the first method (Method1), the seeds are the strongest keypoints assigned by the adopted keypoint detector. Therefore, the number of seeds is given by

$$S_{p1} = K_p \quad (1)$$

K_p is the number of the strongest keypoints obtained by the keypoint detector per image plane p.

After identifying the keypoints as in method1, with the four corners of the image and the keypoints, Delaunay triangles are created with centers that serve as the new seeds for the region-growing algorithm in method2. Since all keypoints except the corners are inside the rectangular convex hull, from the triangulation properties, the number of triangle centroids, which are the seeds method2, is given by

$$S_{p2} = C_p = 2 * K_p + 2 \quad (2)$$

K_p is the number of the detectors' strongest keypoints, and C_p is the number of triangle centers per image plane p.

According to equations (1) and (2), each image's total number of seeds depends on the segmentation method and scheme employed. Consequently, the total number of unique seeds for the GSRG is the same as the number of seeds computed from equations (1) and (2), depending on the method employed. Because only one image plane (i.e., grey level) is used for each image, this is the case.

In contrast, the total number of distinct seed locations for the CSRG scheme could increase to three times the number of seeds computed by equation (1) or equation (2) due to the reason that the SRG segmentation is applied separately to each color plane. So, a single detected keypoint in the CSRG+Method2 scheme could produce up to 12 distinct seed locations (four in each color plane).

Figure 3 depicts the determination of seeds based on either grayscale or color image detection of keypoints with either method1 or method2. In method1, the seeds are the strongly detected keypoints (K_p), whereas, in method2, the seeds are the centers (C_p) of the triangles formed from method1's keypoints. The diagram shows the detected keypoints using SIFT keypoint detection with K_p= 5.

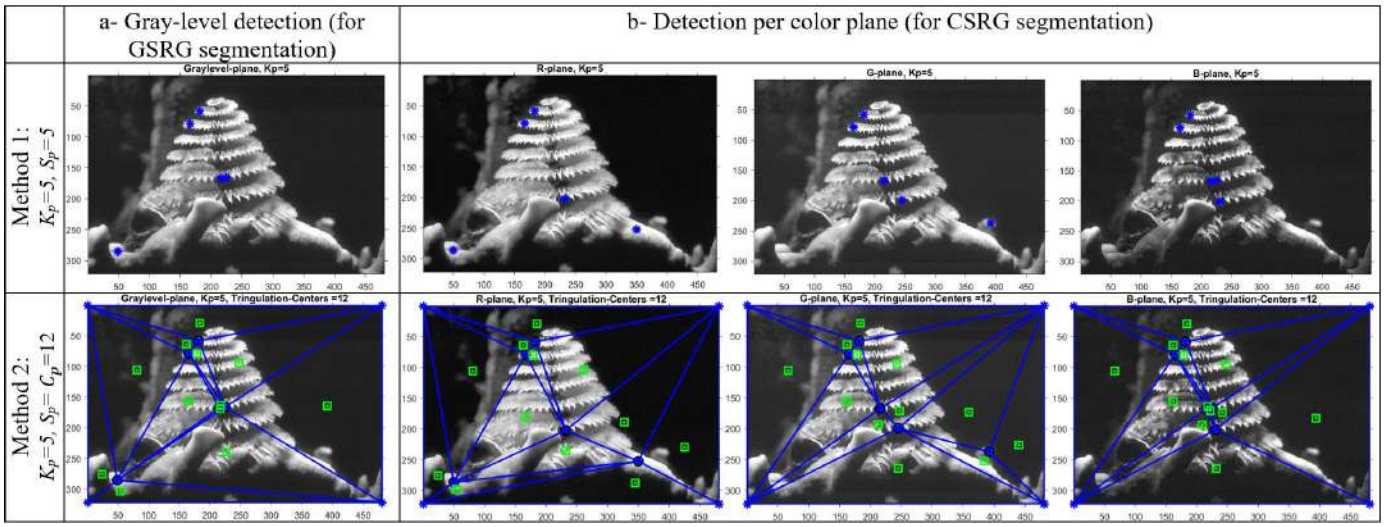

Figure 3. An example of the computed seeds based on: a- Gray-level image keypoints and b- Keypoints detection per color plane. In each case, two methods for calculating the seeds are tested: In method1, the seeds are the strongly detected keypoints (K_p) (blue star markers), whereas in method2, the seeds are the centers (C_p) of the triangles (green square markers), formed from method1's keypoints and image corners.

It is noticed from the illustration of Figure 3 that the seeds are not necessarily located in the exact location among the image color planes, which may increase the number of new seeds' locations for the same image compared to the method of gray-level keypoint detection and may result in better segmentation for a small number of keypoints. Therefore, the total number of distinct seed locations using method2 with the three-color planes may reach up to three times the number of locations of seeds in the gray-level image case.

4. Experimental Results and Discussion

The keypoint-based SRG segmentation schemes described in the previous section are evaluated and assessed using 100 images and their associated ground truth data selected from the 500 images of the Berkely Segmentation Dataset (BSD) [33]. Figure 4 shows a sample of the images from the created 100-image dataset with an example of the ground truth images.

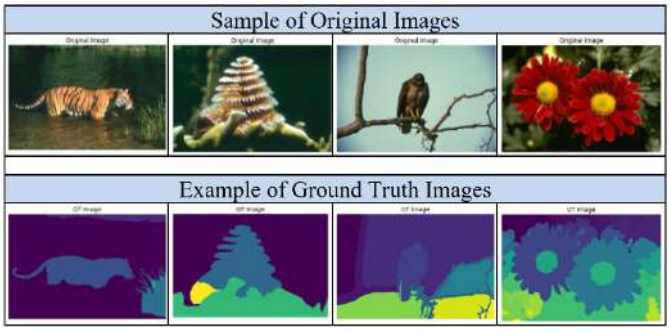

Figure 4. Sample images used in the experiments with a sample of segmentation ground truth.

The region-growing and statistical region-merging MATLAB scripts are adopted and modified for the current experiments from the functions "segCroissRegion" and "srm" found on MATLAB Central File Exchange, respectively. In addition, all keypoint detectors, SIFT, SURF, KAZE, and Harris, are MATLAB functions in toolbox directories.

4.1 Comparing GSRG and CSRG schemes

The mentioned schemes, GSRG and CSRG, are tested with the two methods of seed computation on the given 100-image dataset. Sample of the results of the two methods for obtaining the seeds, as described earlier by method1 and method2, with the two segmentation schemes, GSRG and CSRG, using the SIFT keypoint detector are shown in Figures 5 and 6. For each case, a different number of the obtained strongest keypoints, in which K_p =1, 5, 10, and 20, is examined. Figure 5 shows that the GSRG segmentation improves with the increase of keypoints using method1, while in general, it gives better results for the same number of keypoints with method2. However, in the case of the roses, in the last column, it can be seen that it fails to give a reasonable segmentation outcome. In Figure 6, the other segmentation scheme, CSRG, results in better outcomes than the GSRG segmentation scheme due to using the three-color planes (R, G, and B) in the segmentation process.

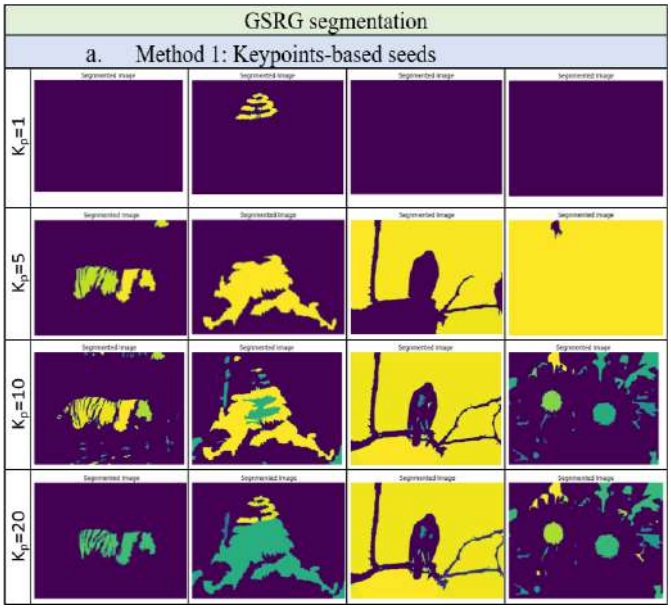

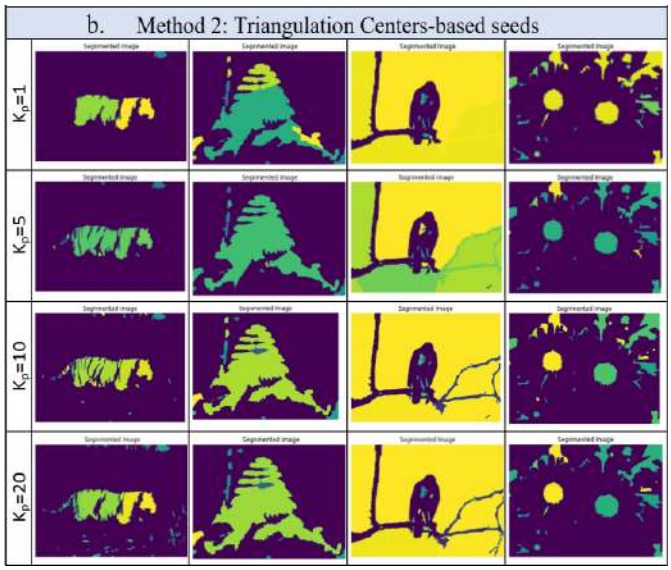

Figure 5. Samples of GSRG segmentation output for method1 and method2 for *Kp*=1,5, 10, and 20.

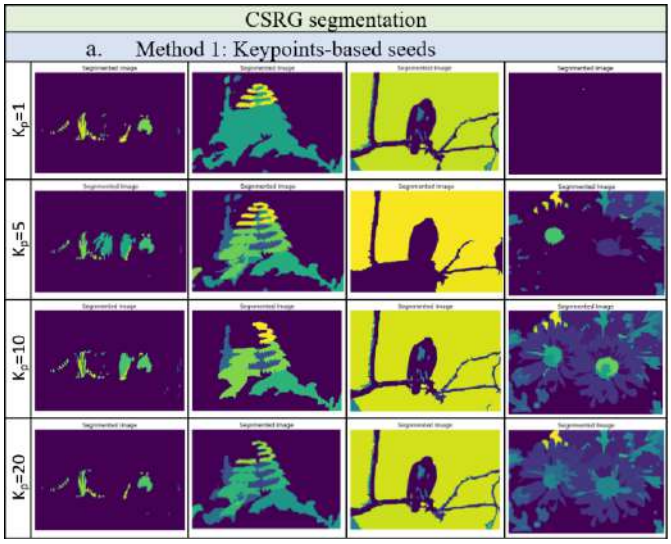

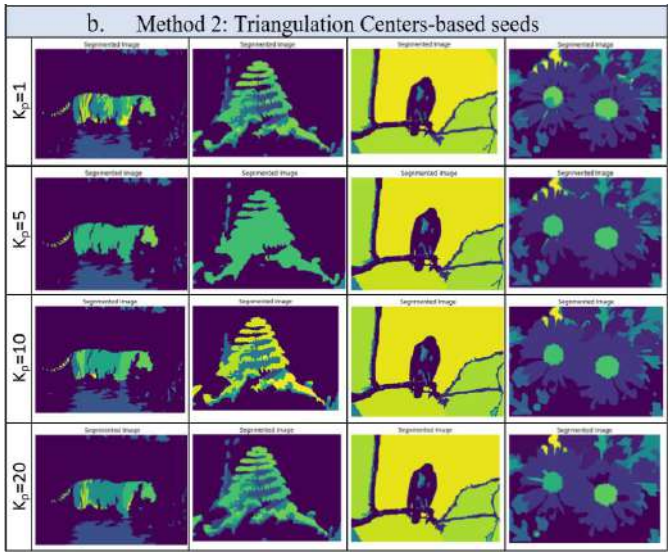

Figure 6. Samples of CSRG segmentation output for method1 and method2 for *Kp*=1,5, 10, and 20.

Two metrics are used to evaluate the segmentation outcome's quality: The first is Segmentation Covering (SC), which evaluates the intersection of segmentation output and ground truth regions [34]. The higher the SC value, the better the quality of segmentation. The Probability Rand Index (PRI) is the second metric, which estimates the probability that a particular pair of pixels has consistent cluster labels. Larger PRI values imply more accurate segmentation results [35], [36].

The statistical merging approach generates multiple segmentation outputs; therefore, three values are computed for each of the two measures: Fixed predicted and ground truth scales (FPGS), through which only the first output of the segmentation outcome and the first ground truth image for each experimental image are considered. Fixed predicted scale (FPS) in which only the predicted scale is fixed with the best match in the ground truth is obtained, and the best scale (Best) finds the best results between the predicted and ground truth images scales.

The results of the segmentation techniques GSRG and CSRG employing the well-known keypoint detection SIFT are shown in Figures 7, 8, 9, and 10, together with the mean SC and mean PRI values for the 100-image dataset. Comparing the results of the mean SC measures for both schemes, GSRG and CSRG, as depicted in Figures 7 and 8, the findings indicate that method2 combined with the CSRG segmentation outperforms the other methods. A similar conclusion may be obtained when comparing the results of the mean PRI measure in Figures 9 and 10. Further, this performance improvement is barely affected by the increase in the number of determined keypoints, particularly for the CSRG scheme, as a result of the increases in the number of image segments and the performance limitations of the statistical region growing method.

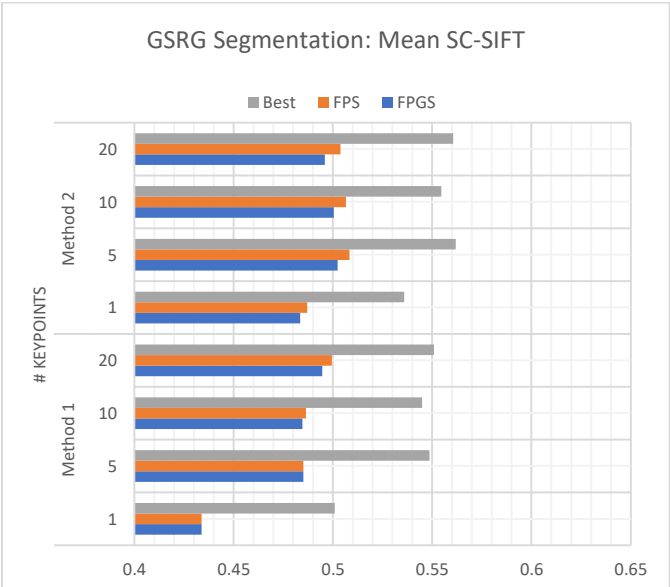

Figure 7. The mean SC results for the segmentation scheme GSRG for the two methods of seeds computation (method1 and method2) using the SIFT keypoint detector.

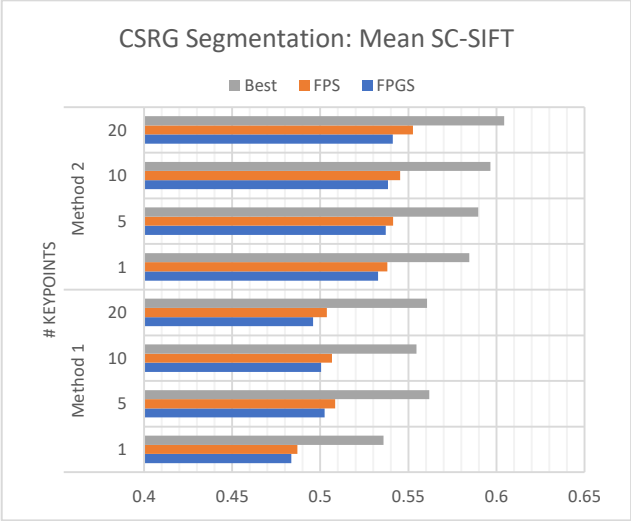

Figure 8. The mean SC results for the segmentation scheme CSRG for the two methods of seeds computation (method1 and method2) using the SIFT keypoint detector.

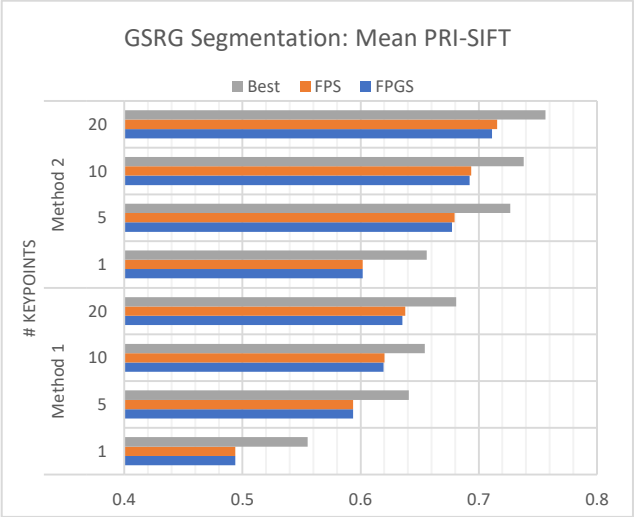

Figure 9. The mean PRI results for the segmentation scheme GSRG for the two methods of seeds computation (method1 and method2) using the SIFT keypoint detector.

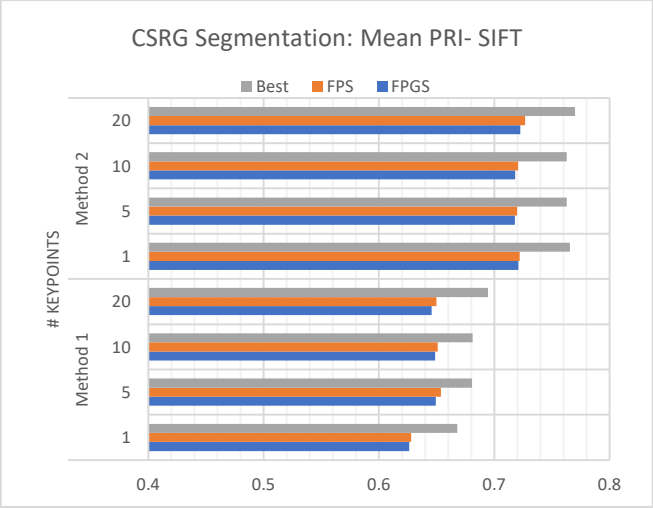

Figure 10. The mean PRI results for the segmentation scheme CSRG for the two methods of seeds computation (method1 and method2) using SIFT keypoint detector.

4.2 Comparing different keypoint detectors

All the experiments and the results shown so far were carried out utilizing the SIFT keypoint detector, one of the famous traditional detectors. However, we need to test the same schemes with different keypoint detectors to see how the performance varies with that change. Therefore, the two extreme settings are chosen to test the SURF, KAZE, and Harris detectors and compare them to the previously tested SIFT detector.

For the lowest configuration, GSRG+Method1 segmentation with a single seed (K_p=1), as shown in Figure 11, the results show that the selection of the keypoint detector may give different segmentation performances, which is due to the difference in locating the assigned seed based on the detection of the strongest keypoint in the grey-level plane of the image. For the highest tested settings of the second scheme, shown in Figure 12, the CSRG+Method2 segmentation scheme is tested with K_p=20 (i.e., S_{p2}= 42 seeds per color plane), the performance of all keypoint detectors improved with a slight lead to the SIFT detector followed by the KAZE detector, then the SURF detector while the Harris detector has the lowest performance among rest.

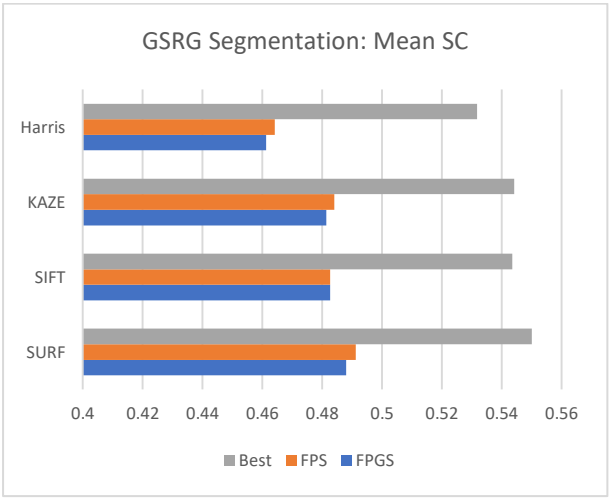

Figure 11. The mean SC measurements for the GSRG+Method1 segmentation with *Kp*=1 using different keypoint detectors.

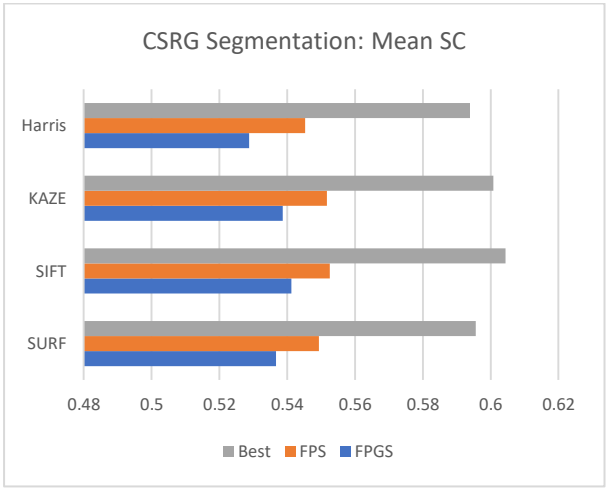

Figure 12. The mean SC measurements for the CSRG+Method2 segmentation with *Kp*=20 using different keypoint detectors.

The other measure, the mean PRI, produces similar leading results for the four tested detectors, as shown in Figure 13 and Figure 14. The differences between these detectors are minor for a large number of seeds and that they are expected to vanish for a much greater number of seeds.

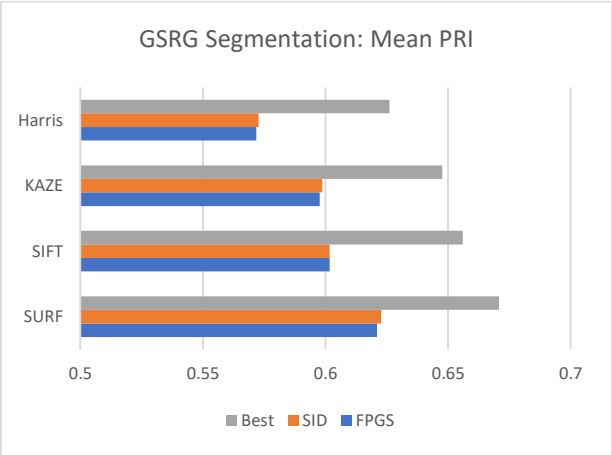

Figure 13. The mean PRI results for the GSRG+Method1 segmentation with Kp=1 using different keypoint detectors.

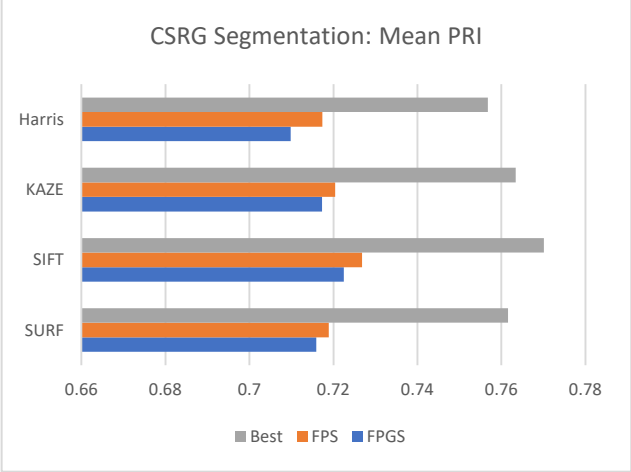

Figure 14. The mean PRI measurements for the CSRG+Method2 segmentation with Kp=20 using different keypoint detectors.

4.3 Comparison with traditional methods

The keypoints-based CSRG segmentation is also compared with other traditional methods widely used in image color reduction and segmentation applications, such as the K-means [37] and the mean shift algorithms [38]. Figure 15 shows a sample of the output of these two algorithms similar to images previously shown in Figures 5 and 6 for visual comparisons with the given algorithms.

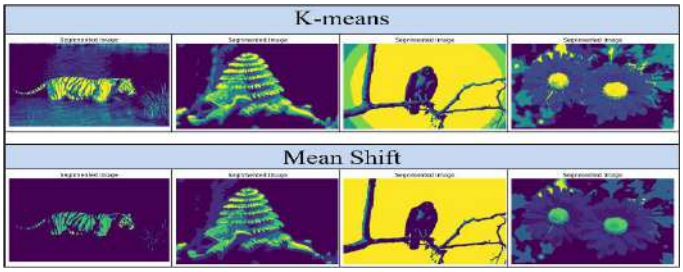

Figure 15. Sample of K-means and mean shift algorithms output for images from the adopted 100 images used in the experiments.

The results of the mean SC and the mean PRI measures in Figure 16 clearly show the differences between the CSRG+Method2 segmentation algorithm compared with the K-means (MATLAB function) and mean shift (MATLAB code implemented by: Bryan Feldman) traditional algorithms.

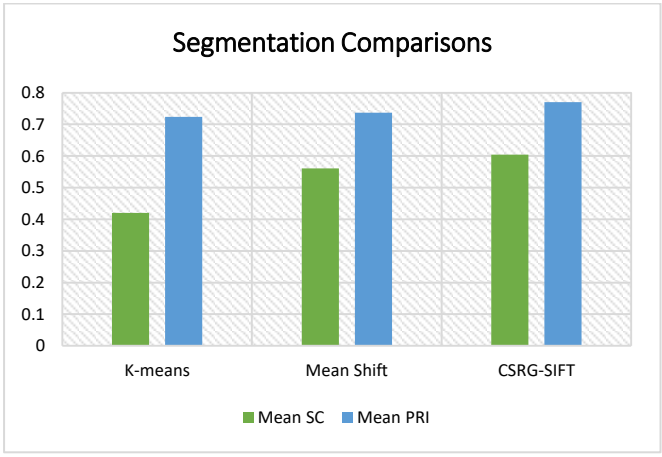

Figure 16. Segmentation comparison between K-means, mean shift, and CSRG+Method2 scheme using the SIFT keypoint detector (with K_p=20 per color plane).

5. Conclusion and Future Scope

The region-growing approaches used for the segmentation of images critically depend on the choice of the seeds to be used. Despite numerous algorithms attempting to manually or automatically select appropriate seeds based on the image's properties or information, keypoint-based seeds provide a suitable solution. A keypoint detector such as SIFT, SURF, KAZE, and Harris may be utilized for allocating the seeds. In instances with fewer seeds, the segmentation results of these detectors may vary based on the detectors' locations identified by the detector. However, if there are many determined seeds, the segmentation results may not directly reflect the effect of adopting a particular keypoint detector. Finding the centroids of the triangulations created by the strongest detected keypoints for each color plane in the given image is one method to increase the number of seeds while preserving coverage of the image's essential regions. In addition, utilizing SRM, which merges analogous segments, enhances the performance of the segmentation.

The findings could be improved by identifying other seeds; necessitating increased computational complexity. Therefore, future research may concentrate on eliminating irrelevant seeds and limiting duplication. Additionally, alternative methods of growing regions, particularly those that provide a more adaptive combination and aggregation of regions based on the properties of each image part, could be studied.

References

[1]. H. Mittal, A.C. Pandey, M. Saraswat, et al. "A comprehensive survey of image segmentation: clustering methods, performance parameters, and benchmark datasets." *Multimedia Tools Appl.*, Vol. **81**, pp. **35001–35026, 2022**. https://doi.org/10.1007/s11042-021-10594-9

[2]. Shaik Salma Begum, D. Rajya Lakshmi, "A Review of Current Methods in Medical Image Segmentation," *International Journal of Computer Sciences and Engineering*, Vol.**7**, Issue.**12**, pp.**67-73**, **2019**. https://doi.org/10.26438/ijcse/v7i12.6773

[3]. R. Yadav, M. Pandey, "Image Segmentation Techniques: A Survey." In: Gupta, D., Polkowski, Z., Khanna, A., Bhattacharyya, S., Castillo, O. (eds) *Proceedings of Data Analytics and Management. Lecture Notes on Data Engineering and Communications Technologies*, Vol **90**., pp. **231-239**, **2022**, Springer, Singapore. https://doi.org/10.1007/978-981-16-6289-8_20

[4]. N. J. Wala'a, J. M. Rana, "A Survey on Segmentation Techniques for Image Processing," *Iraqi Journal for Electrical and Electronic Engineering*, Vol. **17**, pp. **73-93**, **2021**, doi:10.37917/ijeee.17.2.10

[5]. N. Zeitoun, M. Aqel, "Survey on image segmentation techniques", *Procedia Computer. Sci*., Vol.**65**, pp. **797-806**, **2015**. https://doi.org/10.1016/j.procs.2015.09.027.

[6]. R. Adams, L. Bischof, "Seeded Region Growing," *IEEE Transactions on Pattern Analysis and Machine Intelligence*, Vol. **16**, No. **6**, pp. **641-654, 1994**. DOI:10.1109/34.295913

[7]. M. Mousavi, F. Shariaty, M. Orooji, E. Velichko, "The performance of active-contour and 445 region growing methods against noises in the segmentation of computed-tomography scans," in *International Youth Conference on Electronics*, *Telecommunications and Information Technologies. Springer*, Vol. **255**, pp. **573–582**, **2021**. https://doi.org/10.1007/978-3-030-58868-7_63

[8]. M. Mancas, B. Gosselin, B. Macq, "Segmentation using a region-growing thresholding," *Image Processing: Algorithms and Systems IV*, Proc. SPIE Vol. **5672**, (1 March **2005**); https://doi.org/10.1117/12.587995

[9]. J Borovec, J Kybic, A Sugimoto, "Region growing using superpixels with learned shape prior," *Journal of Electronic Imaging,* Vol.**26**, No. **6**, **2017**. https://doi.org/10.1117/1.JEI.26.6.061611

[10]. A. Callara, C. Magliaro, A. Ahluwalia, N. Vanello, "A Smart Region-Growing Algorithm for Single-Neuron Segmentation from Confocal and 2-Photon Datasets", *Front. Neuroinform,*. Vol. **14:9**, **2020**. DOI: 10.3389/fninf.2020.00009

[11]. O. Al-Furaiji, V. Rabtsevich, V. Tsviatkou, T. Kuznetsova, S. Chizhik, "Segmentation of AFM-Images Based on Wave Region Growing of Local Maxima," *Engineering Letters*, Vol. **28**, no.**3**, pp. **681-698**, **2020**.

[12]. N. Muhadi, A. Abdullah, S. Bejo, M. Mahadi, A. Mijic, "Image Segmentation Methods for Flood Monitoring System," *Water*, Vol. **12**, no. **6**, pp. **1825**, Jun. **2020**, doi: 10.3390/w12061825.

[13]. H. Wang, Y. Chen, "A smoke image segmentation algorithm based on rough set and region growing," *Journal of Forest Science*, Vol. **65**, pp. **321-329**, **2019**. doi: 10.17221/34/2019-JFS

[14]. X. Jiang, Y. Guo, H. Chen, Y. Zhang, Y. Lu, "An Adaptive Region Growing Based on Neutrosophic Set in Ultrasound Domain for Image Segmentation," *IEEE Access*, vol. **7**, pp. **60584-60593**, **2019**, doi 10.1109/ACCESS.2019.2911560.

[15]. Y. Deng and B. S. Manjunath, "Unsupervised segmentation of color-texture regions in images and videos," *IEEE Trans. Pattern. Anal. Mach. Intell.*, vol. **23**, no. **8**, pp. **800-810**, Aug. **2001**.

[16]. F. Jing, M. Li, H. J. Zhang, and B. Zhang, "Unsupervised image segmentation using local homogeneity analysis," in *Proc. Int. Symp. Circ. Syst*., **2003**. DOI:10.1109/ISCAS.2003.1206008

[17]. J. Fan, D. K. Y. Yau, A. K. Elmagarmid, and W. G. Aref, "Automatic image segmentation by integrating color-edge extraction and seeded region growing," *IEEE Trans. Image Process.*, Vol. **10**, no. 10, pp. **1454-1466**, Oct. **2001**.

[18]. I. Imtiaz, I. Ahmed, M. Ahmad, K. Ullah, A. Adnan, M. Ahmad, "Segmentation of Skin Lesion Using Harris Corner Detection and Region Growing," *2019 IEEE 10th Annual Ubiquitous Computing, Electronics & Mobile Communication Conference (UEMCON)*, New York, NY, USA, pp. **0614-0619**, **2019**. DOI: 10.1109/UEMCON47517.2019.8993034.

[19]. F. Y. Shi, S. Cheng, "Automatic seeded region growing for color image segmentation," Image Vis. Compt., vol. **23**, pp. **877- 886**, **2005**.

[20]. J. Fan, G. Zeng, M. Body, M. Hacid, "Seeded region growing: an extensive and comparative study," Pattern Recognition Letters, Vol. 26, Issue 8, Pages 1139-1156, **2005**. https://doi.org/10.1016/j.patrec.2004.10.010

[21]. L G. Ugarriza, E. Saber, S. R. Vantaram, V. Amuso, M. Shaw, R. Bhaskar, "Automatic image segmentation by dynamic region growth and multiresolution merging," IEEE Trans. Image Process., Vol. **18**, no. **10**, pp. **2275-2288**, Oct. **2009**.

[22]. C. -C. Kang and W. -J. Wang, "Fuzzy based seeded region growing for image segmentation," NAFIPS 2009 - 2009 Annual Meeting of the North American Fuzzy Information Processing Society, Cincinnati, OH, USA, pp. **1-5**, **2009**. DOI: 10.1109/NAFIPS.2009.5156397.

[23]. A. Al-Faris, U. Ngah, N. Isa, I. Shuaib, "Breast MRI tumour segmentation using modified automatic seeded region growing based on particle swarm optimization image clustering." In Proceedings of the Advances in Intelligent Systems and Computing; Springer Verlag, Vol. **223**, pp. **49–60**, **2014**.

[24]. H. Tariq, T. Jilani, U. Amjad. S.M. Aqil Burney, "Novel Seed Selection and Conceptual Region Growing Framework for Medical Image Segmentation." BRAIN – Broad Research in Artificial Intelligence and Neuroscience, Vol. **10**, Issue **1**, **2019**, ISSN 2067-3957.

[25]. N. Tuan, X. Dai, T. Yurevich, "Multiple Seeded Region Growing Algorithm for Image Segmentation Using Local Extrema," Minsk, Belarus, January **2021**.

[26]. H. Shimodaira, "Automatic color image segmentation using a square elemental region-based seeded region growing and merging method." arXiv preprint, arXiv:1711.09352, **2017**. https://doi.org/10.48550/arXiv.1711.09352

[27]. N. Jothiaruna, K. Joseph Abraham Sundar, B. Karthikeyan, "A segmentation method for disease spot images incorporating chrominance in Comprehensive Color Feature and Region Growing." Computer. Electron. Agric. Vol **165**, **2019**. https://doi.org/10.1016/j.compag.2019.104934

[28]. J. Jiao, X. Wang, J. Zhang, Q. Wang, "Salient region growing based on Gaussian pyramid," IET Image Process., Vol. **15**, Issue **13**, pp. **3142– 3152**, **2021**. https://doi.org/10.1049/ipr2.12307

[29]. D. G. Lowe, "Distinctive image features from scale invariant keypoints," International Journal of computer vision, Vol. **60**, no. **2**, pp. **91–110**, **2004**.

[30]. H. Bay, A. Ess, T. Tuytelaars, L. Van Gool, "Speeded-Up Robust Features (SURF)," Computer Vision and Image Understanding, Vol. **110**, Issue **3**, pp. **346-359**, **2008**. https://doi.org/10.1016/j.cviu.2007.09.014

[31]. P. F. Alcantarilla, A. Bartoli and A. J. Davison, "Kaze features," European Conference on Computer Vision. Springer, In: Fitzgibbon, A., Lazebnik, S., Perona, P., Sato, Y., Schmid, C. (eds) Computer Vision – ECCV 2012. Lecture Notes in Computer Science, Springer, Berlin, Heidelberg, Vol **7577**. pp. **214–227**, **2012**. https://doi.org/10.1007/978-3-642-33783-3_16

[32]. C. Harris, M. Stephens, "A Combined Corner and Edge Detector," Proceedings of the 4th Alvey Vision Conference, pp. **147-151**, August **1988**.

[33]. P. Arbeláez, M. Maire, C. Fowlkes, and J. Malik, "Contour Detection and Hierarchical Image Segmentation," IEEE Transactions on Pattern Analysis and Machine Intelligence, Vol. **33**, no. **5**, pp. **898-916**, May **2011**. DOI: 10.1109/TPAMI.2010.161.

[34]. T. Malisiewicz, A. Efros, "Improving Spatial Support for Objects via Multiple Segmentations," *Proceedings of the British Machine Vision Conference **2007***, University of Warwick, UK, September **10-13**, **2007**. ISBN 1-901725-34-0.

[35]. Unnikrishnan, Ranjith, and Martial Hebert. "Measures of Similarity." *Seventh IEEE Workshops on Applications of Computer Vision (WACV/MOTION'05)* – Vol. **1**, pp. **394-394**, **2005**.

[36]. R. Unnikrishnan, C. Pantofaru, M. Hebert, "Toward objective evaluation of image segmentation algorithms," *IEEE Trans.*

Pattern Anal. Mach. Intell., Vol. **29**, no. **6**, pp. **929–944**, Jun. **2007**.

[37]. S. K. Khan, A. Ahmad, "Cluster center initialization algorithm for k-means clustering," *Pattern Recognition Letters*, Vol. **25**, Issue **11**, pp.**1293–1302**, **2004.** https://doi.org/10.1016/j.patrec.2004.04.007.

[38]. D. Comaniciu, P. Meer, "Mean shift: a robust approach toward feature space analysis," *IEEE Transactions on Pattern Analysis and Machine Intelligence*, vol. **24**, no. **5**, pp. **603-619**, May **2002**. doi: 10.1109/34.1000236.

AUTHORS PROFILE

Ibrahim El rube' (IEEE M'07, SM'12) received a B.Eng. degree from the computers and electronics engineering department in 1992, the M.Sc. degree in Electronics and communications engineering in 1999 respectively, from the AASTMT, Egypt, and the Ph.D. degree in systems design engineering from the University of Waterloo, in 2006, Canada. He has held lecturing positions at the Department of Electronics and Communications Engineering, AASTMT, Egypt, during the years from 1993 to 2011. In Aug. 2006, he became an Assistant Professor, and an Associate Professor in 2010. In 2011, he joined the computer engineering department at Taif University, where he is currently an Associate Professor. His research interests include signal and image processing, computer vision, pattern recognition, and machine learning.

